ChemComm

Recent Advancements in Understanding the Self-assembly of Macroions in Solution via Molecular Modeling

Journal:	*ChemComm*
Manuscript ID	CC-FEA-08-2022-004535.R1
Article Type:	Feature Article

ARTICLE

Received 00th January 20xx,
Accepted 00th January 20xx

DOI: 10.1039/x0xx00000x

Recent Advancements in Understanding the Self-assembly of Macroions in Solution via Molecular Modeling

Zhuonan Liu[a,†], Kun Qian[a], Tianbo Liu[a] and Mesfin Tsige[a]

Macroionic solutions behave quite differently from small ions in solution or colloids in suspension, representing a previously missing and very important transitional stage, and can further be connected to solutions of polyelectrolytes, including proteins and DNA (e.g., similarities between "blackberry" formation and virus capsid formation). While synthesis and characterization have produced an immense database regarding the self-assembly behavior of macroions in solution resulting in many empirical rules and guidelines, theory and simulations are sorely needed to connect these disparate threads into a cohesive and coherent narrative of macroionic solution theory and to provide guidance for future work. We recently developed a versatile coarse-grained model specifically designed for modelling the self-assembly of macroions in solution and have answered some of the most outstanding questions about the solution behavior of macroions including the source of the attractive force between like-charged macroions and how they self-assemble into a 2D monolayer structure.

1. Introduction

Solutions of hydrophilic macroions represent a transition stage between simple ions and large colloids. It has been found that such macroions have completely different solution behavior from the other two systems and could represent a previously missing intermediate region between them. Soluble inorganic ions are expected to distribute homogeneously in dilute aqueous solutions. However, this widely accepted concept does not seem to hold for some giant, highly soluble, hydrophilic macroions carrying moderate amount of charges, such as polyoxometalate (POM)[1-4] and POSS[5-7] anions, metal-organic cations[8-10], small nanoparticles and charged dendrimers[11-14] (see Fig. 1). POMs are a large group of nanometer-scaled metal-oxide molecular clusters and their derivatives[15-29] with well-defined molecular structure, uniform size, shape, mass and (in certain range) adjustable charge density. The cationic metal-organic cages (MOC)[30,31] are formed by transition metal cations interacting with special organic ligands to form well-defined structures. Other examples of macroions include charged dendrimers, soluble small nanoparticles, as well as biomacromolecules. These macroions tend to attract with each other and often self-associate into hollow, spherical, single-layer, vesicle-like blackberry-type structures in dilute solutions (see Fig. 1)[32-34].

The macroions cannot be described by the Debye-Hückel Theory because they cannot be treated as point charges, while on the other

[a] School of Polymer Science & Polymer Engineering, The University of Akron, Akron, OH, 44325, USA.
† Currently at 3M

hand they are still soluble and form "real solutions" which distinguishes them from colloids. Such macroions can also serve as a model to the poorly understood polyelectrolyte (including biomacromolecular) solutions.

On the experimental side, Liu et al. has formulated the following important conclusions and hypothesis using various techniques including static and dynamic light scattering (SLS and DLS), transmission and scanning electron microscopes (TEM and SEM), solution nuclear magnetic resonance (NMR) spectroscopy, Zeta potential Analysis, small-angle X-ray scattering (SAXS), isothermal titration calorimetry and analytical ultracentrifugation:

(1) Hydrophilic macroions soluble in water or other polar solvents can strongly attract each other and form hollow, spherical, single-layer structures (known as "*blackberry*" structures) when carrying moderate amount of charge.[36-39]

(2) The counterion-mediated attraction is the major driving force for the self-assembly, while the van der Waals (vdW) forces are negligible[36,40-43].

(3) Tuning the charge density of macroions (or the solvent composition) leads to the transition between the single macroions and the blackberry structures[44], as well as changes in the blackberry size. The blackberry size decreases monotonically with increasing macroionic charge density (or increasing solvent polarity, measured in dielectric constant) until the blackberries disintegrate to single macroions[36].

(4) The interaction (consequently the blackberry formation and size) between the macroions and their counterions is controlled by the valence and hydration shell of counterions. Among the monovalent counterions, the ones with smaller hydration shells will be associated with the macroions first. Counterion replacement (even among monovalent ions) around macroions can be achieved.[45]

(5) The blackberry formation in dilute solutions could be very slow (takes weeks to months) to reach equilibrium at room temperature, due to the very difficult dimer and oligomer formation process. The whole process accelerates with time. The overall kinetic curve (sigmoidal curve) is similar to that of virus capsid formation denoting the existence of templated self-recognition.[46]

(6) The blackberry formation demonstrates an amazing self-recognition behaviour. Two types of macroions in the same solution can strictly self-recognize with each other and form two types of individual blackberries instead of mixed ones.[47,48] This can even be achieved between two macroionic enantiomers.

It is very important to correlate the well-established experimental understanding of macroionic solutions with strong theoretical and simulation studies.

Theoretical and simulation-based modeling of POMs to date has primarily been focused on their electronic properties, rather than their solution features.[49-84] Many of the theoretical investigations of POMs to understand their electronic properties have taken advantage of quantum chemistry methods, mainly Density Functional Theory (DFT)-based methods.[54-56,58,59,65,72,76] Ideally, full configuration interaction calculations with large basis sets can approach exact solutions of the Schrödinger equation for certain systems, but the number of calculations can scale exponentially with the system size, whereas DFT-based methods can give accurate (but comparatively less precise) with a greater computational efficiency. At the same time, for both these approaches, only system sizes in the hundreds of atoms are typically the largest that can be feasibly performed on the traditional parallel computing platforms. For macromolecular systems, then, it is more common to model isolated molecules or representative segments of molecules than to simulate

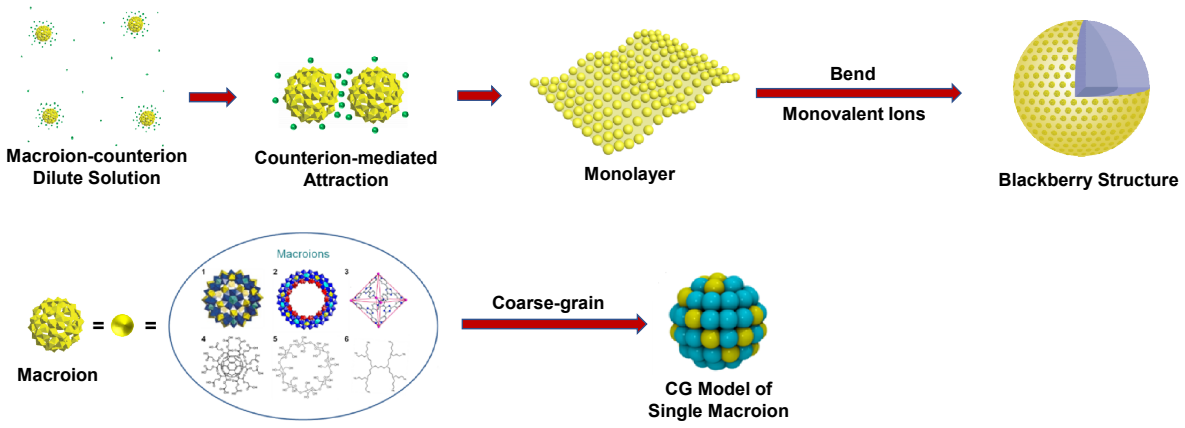

Figure 1. (top) Cartoon representing the self-assembly process in finally forming a "blackberry" structure in solution. (bottom) Some typical macroions, including inorganic metal-oxide molecular clusters (1, 2), metal-organic nanocages (3), functionalized fullerenes (4), cyclodextrins (5), dendrimers (6) [35]. A coarse-grained model designed for general spherical macroions is shown on the right side. In this model, the cyan beads have only vdW interactions while the yellow beads have both vdW and electrostatic interactions.

entire arrays of macromolecules in solvent or adsorption interactions.

Investigation through Molecular dynamics (MD) simulation of macroions assembly in solution is expected to overcome some of the limitations in system size and accessible time scale. On the detailed side of MD simulation are all-atom simulations (all-atom MD), which forgo the electronic-structure specificity of quantum simulation for a representation based on individual atoms and the interactions between them. All-atom MD has been used to study macroions in solutions – including the diffusion of macroion molecules in solution and the distribution of water molecules and counterions around them.[85-88] Tsujimichi et al. in 1995 used a force field developed for other metal oxides to study the structure of the solvent (water) around $[PMo_{12}O_{40}]^{3-}$ with three K^+ counterions – to the best of our knowledge this was the first classical simulation of a POM in an explicit solvent.[85] However, the simulation time was only a few picoseconds long, resulting in poor statistics and made it hard to draw a definitive conclusion on the structure of the solvent around the POM. In 2005, Lopez et al. gave a clear picture of the structure of the solvation shell by simulating $[PW_{12}O_{40}]^{3-}$ and three Na^+ counterions in water and running the system for relatively long time with a simulation time of 2 ns.[87] Leroy et al. used the same method to show that the dynamic behavior of the macroions was strongly dependent on ion-pairs in the first solvation shell while the ion-pairs in the second solvation shell may also have important consequences.[88]

Wipff did the only work so far on the aggregation of macroions (up to 20) in solution using all-atom simulation and identified the formation of oligomers (from dimers up to pentamers) within a simulation time of 20 ns.[89,90] This work proved that there is indeed attractive interaction between POM macroions. However, due to the limitations in what can be achieved through all-atom simulations and available computational capability, these studies handled only small systems at very high concentrations, leading to less conclusive but still relevant results on the self-assembly behavior of macroions in solution. In general, basic all-atom MD is capable of accessing time scales on the order of tens of nanoseconds but becomes difficult for very large systems or for dynamics expected to take place over very long-time scales such as the self-assembly of macroions.

Given that macroions fill the gap between simple ions and colloids in size but display a completely different self-assembly behavior, there was a reasonable amount of interest from the simulation community about a decade ago to understand this unique class of system as highlighted above. Unfortunately, the time and length scales involved in the self-assembly process of macroions in solution became a bottleneck for many of the previous simulation attempts that used either DFT or all-atom simulation approaches. This significantly hampered the in-depth and scope of questions and analysis that could be done through simulations. The principal role of simulations in the field of macroions have thus been in interpreting experimental results. To overcome these challenges, we recently developed a coarse-grained (CG) model specifically designed to study the self-assembly behavior of macroions in solution[91,92]. The model allows simulating mesoscale physical processes while retaining the molecular details of the system.

CG simulation methods in general attempt to circumvent the difficulties associated with small time steps and length scales in all-atom simulation by combining atoms into “superatoms” called “beads”. One advantage is that the very fast motion associated with bond fluctuations is largely avoided and thus a larger time step can be chosen. This can either be used to perform simple simulations much more quickly or to extend the range of accessible time scales from ns to μs or even ms. Furthermore, the reduction in the system’s degrees of freedom allows one either to simulate the same system with fewer particles for less computational overhead or to simulate much larger systems using the same number of particles to probe much larger length scales. The versatility of our model also allows for modifications or additions to the potentials that can recreate interactions like hydrogen bonding without being limited to a specific chemistry.

In this Feature article, we summarize the recent advances we have made in the fundamental understanding of the self-assembly of macroions in solution using our CG model.

2. Modelling and Simulation Details

To study the general self-assembly behavior of various hydrophilic macroions, a flexible coarse-grained (CG) model that represents macroions of varying charge and size was developed[91,92]. The design of the CG model is based on the molecular structure of typical macroions such as polyoxometalate molecules. One macroion is represented by one hollow sphere with two different types of beads on the surface (see Fig. 1). The surface beads are either uncharged or charged to represent the van der Waals and electrostatic interactions among macroions, counterions and solvent molecules in the solution. The size and charge value of each surface bead, the size of the macroion, and the number of charged beads and their distribution on the surface can all be tuned to represent a specific type of macroion. Many macroions, such as {Mo72Fe30} and C60, have localized charges and hence the charges on the surface of macroions in our model are treated to be localized.

The Lennard-Jones (LJ) 12-6 potential energy function was used to describe the van der Waals interactions between different kinds of species in the solution. The CG force field parameters for solvent were taken from the model of water in MARTINI force field[93]. In this CG model of water, one bead is equivalent to four water molecules. The CG beads on the surface of macroions also have the same size (5 Å), σ, and van der Waals interaction parameters, ε, as the solvent beads to account for their hydrophilic characteristic, so are the counterions. While reduced units are used in our CG model, the following conversion is used in translating the reduced units to real units so that the reader can have a sense of the simulation time and length scales accessed through our current simulations[91]. In our CG model, the ε of all pair interactions between all kinds of species is set to 4.5 kJ/mol, and the σ is set to 5 Å to obtain a good solvent

environment. The cut-off distance r_c is set to 15 Å for all LJ interactions.

Furthermore, the interactions between the different charged beads were described by the Coulomb pair-potential. In the work reported here, each charged bead on the surface of macroions has one negative charge, and accordingly each counterion has one positive charge, while the solvent beads are not charged.

Though the interaction between a macroion bead and a solvent bead was set to be identical to that between two solvent beads in most of the work we have done so far, the proposed coarse-grained model is, however, versatile and can capture the different possible dispersion interactions between macroions and solvents. This can be performed by tuning the LJ parameters ε and σ between all relevant macroion bead-solvent bead pairs allowing for a reliable representation of solvent quality as good, neutral, or bad. Furthermore, the different LJ sites on the surface of the macroions can be assigned either identical or different LJ parameters to study homologous and heterogeneous interactions of macroions and/or macroions and solvents. This allows us to capture the different asymmetries that exist in the different types of macroions that have been investigated by experimentalists. Using this approach, we have validated our proposed model, interpreted existing experimental data, and guided the design of new experiments and some of them are presented below.

3. Solution Properties of Hydrophilic Macroions

The coarse-grained model for macroions we developed has been found to be helpful in providing a general understanding of various soluble, hydrophilic macroionic solutions; especially the strong attraction among the like-charged soluble macroions and the consequent spontaneous, reversible formation of hollow, spherical, single layer, vesicle-like blackberry-type structure with tuneable sizes. The results hold great promise in our understanding of macroionic solutions from empirical experience to general rules.

3.1. Source of the attractive force between macroions[91]: Our initial investigation was focused on answering the following question: what is the source of the attractive force among like-charged soluble macroions with moderate charge density and monovalent counterions—in the absence of chemical interaction and hydrogen bonding?

To answer this question, we investigated the interaction between two isolated 2.5-nm-diameter charged macroions in dilute solution. It took more than 250 ns for the two macroions, that were initially separated by 20 nm in the solution, to form a stable pair, which we will refer it hereafter as dimer. Both the van der Waals and electrostatic interactions are favourable for dimer formation as shown in Figure 2a and 2b, respectively. The contribution of the van der Waals interaction to the dimer formation is, however, about four orders of magnitude smaller than the contribution of the electrostatic interaction. Due to screening by the counterions, the electrostatic interaction between the two macroions displays a short-range behavior, similar to the van der Waals interaction. We believe that is why it took so long to form the dimer state.

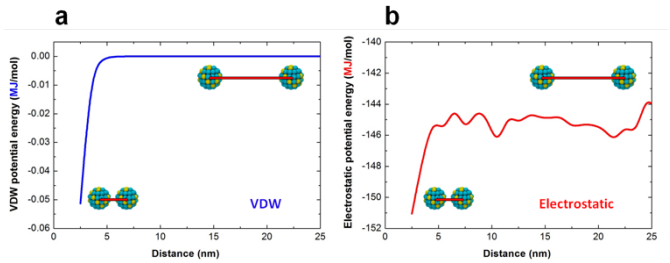

Figure 2. Comparison of two types of potential energy between macroions and counterions. (a) The van der Waals potential energy of the two macroions as a function of the distance between them. (b) The electrostatic potential energy as a function of the distance between two macroions.

To confirm that electrostatic interaction is mainly responsible in the self-assembly of macroions in solution, a system containing 27 charged, 2.5 nm-diameter, macroions in solution was simulated. The macroions self-assembled into a single aggregate as shown in Figure 3b within 500 ns. This further confirms that like-charged macroions attract one another in solution to form one big aggregate mediated by counterions. A similar system, but with uncharged macroions and no counterions was also simulated to determine the role of van der Waals interactions in the self-assembly process. As shown in Figure 3e, no sign of any kind of aggregation, even at a dimer level, was observed after simulation of more than 500 ns. This confirms our earlier observation that van der Waals interactions do not play a significant role in the self-assembly of like-charged macroions in solution. This begs the question, what would happen to the aggregate shown in Figure 3b if the electrostatic interactions are turned off and the simulation is continued? The simulation proved that the aggregate immediately, within a few picoseconds, disassembled into isolated macroions as shown in Figure 3c.

The simulation results presented above confirm experimental observations that counterion-mediated electrostatic attraction between macroions is the major driving force for the self-assembly of macroions in solution. However, note that the self-assembly shown in Figure 3b is a not two-dimensional (2D) monolayer and this was investigated further and is presented below.

3.2. The fundamental reason behind the symmetry-breaking phenomenon during the self-assembly of macroions in solution[92]: The most intriguing question is why the macroions assemble into hollow (i.e. two dimensional), spherical structures? Many types of macroions, such as the Keplerates, C_{60} and some MOCs, are structurally isotropic, which is different from the structurally anisotropic surfactants. To form the hollow, spherical blackberry structure, the macroions need to have stronger intermolecular attraction along certain directions in a homogeneous bulk solution. That means, a symmetry-breaking process should take place, but how that happens has been a major mystery until our recent

simulation result provided a convincing answer to it.

Although it is computationally unfeasible to simulate the formation of a blackberry structure because it may contain thousands of single macroions; it is, however, possible to simulate the early stage of the self-assembly behavior since the macroions should initially self-assemble into a 2D monolayer before forming the blackberry-like structure. Simulation of different systems containing 27 macroions or more with moderate charges randomly distributed on the surface of the macroions resulted in a 3D aggregate similar to Figure 3b. This matched our expectation given that there should not be any directional preference for the self-assembly because the macroions were assigned random charge distribution on their surface.

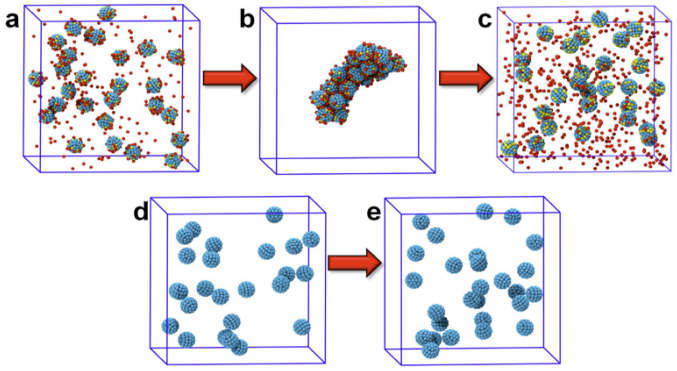

Figure 3. Snapshots of charged and uncharged macroions in solution: (a, d) at the beginning and (b, e) at the end of the simulations, respectively. Charged beads on macroions are colored in yellow, while uncharged beads on macroions are colored in cyan, and charged counterions are colored in red. (c) shows the final outcome after turning off all the charges to the aggregate shown in (b) and running the simulation further with no Coulomb interactions. Solvent beads are not shown in all the snapshots for clarity.

Since many macroions have rigid structures, we hypothesized that the positions of the charged sites on the macroions may be reconfigured depending on the solution environment to break the isotropic symmetry and self-assemble into a 2D monolayer structure. That means, though many macroions are structurally isotropic, the charge distribution on their surface in a solution may not necessarily be isotropic.

To verify our hypothesis, systems containing a large range of charge densities and charge distributions on macroion surfaces were simulated. Eight representative macroions with moderate charge densities and different charge distributions are shown in Figure 4a-h. From the simulations, we discovered that only a selected group, those with charges distributed close to what we refer to as the "equator" (Figure 4d, e and f) of the macroions, self-assembled into 2D monolayers while the rest assembled into a 3D aggregate[92]. Representative 2D monolayers are shown in Figure 4i and 4j which show the macroions packed in a well-defined hexagonal structure that is in excellent agreement with recent experimental observation. In the experiments[94,95], they showed that standalone 2D nanosheets are formed by two types of macroions: 2.5-nm spherical $\{U_{60}\}$ peroxide clusters and 2-nm-size metal-organic cage in dilute solutions.

3.3. Thermodynamic justification for the preferred type of charge distribution on the surface of macroions[92]: The self-assembly of macroions is not entropically favourable since the entropy is reduced due to the macroions self-assembling into a well-defined structure. In other words, enthalpy should be the driving force that lowers the free energy of the solution during the self-assembly of macroions. From our simulations of several batches of different macroionic solution systems, where for each batch the systems were identical except the distribution of the charges on the surface of the macroions, we found that systems with macroions having charges distributed close to their "equator" have the lowest enthalpy, i.e. energetically favourable, after forming stable assembled structure[92]. So, in solution, we hypothesize that macroions would prefer to have their charges distributed around the equator to minimize the system free energy.

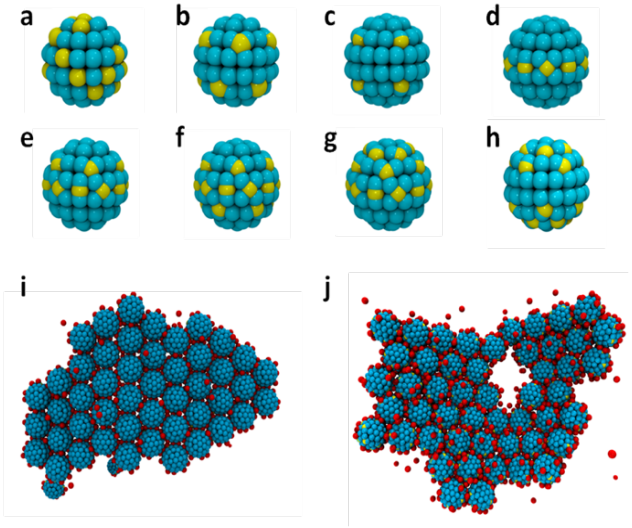

Figure 4. CG models of macroions with various charge distributions and 2D monolayer structures formed by certain types of macroions. The charge distributions of the CG models are: (a) 20 charges randomly distributed on the surface; (b) 10 charges on the "tropics" (analogous to a globe); (c) 8 charges on the vertices of a cube (body diagonal 2.5 nm); (d) 10 charges on the "equator"; (e) 15 charges on the equator and one tropic; (f) 20 charges on the equator and both tropics; (g) 20 charges on half sphere; (h) 20 charges on top and bottom. (i) Final assembly of macroions with a charge distribution shown in d. (j) Final assembly of macroions with a charge distribution shown in f. All the macroions are 2.5 nm in size. Solvent molecules are not shown in i and j for clarity.[92]

These results imply that the charge distribution on the surface of macroions in solution may be dynamic, that is

redistributing closer to the macroion's equatorial area to achieve the lowest energy state of the solution. This intriguing result from simulation has been very hard to directly confirm through experiment. The immediate question we got from our experimental collaborator Liu's group was, why macroions such as Keplerate, with apparently isotropic charge distribution, also self-assemble into 2D monolayers prior to the blackberry structure formation? To answer this question, we designed a model macroion where 30 negative charges were symmetrically assigned on the 30 vertices of an icosidodecahedron surface shown in Figure 5d that is identical to the locations of possible charge sites on the surface of $\{Mo_{72}Fe_{30}\}$ (a 2.5-nm diameter spherical cluster). Such macroions also forming a 2D monolayer as shown in Figurer 5a-c was surprising to us. The macroions pack in hexagonal close-packed structure, like the ones with charges distributed close to their equators. This is very interesting because our model correctly captures what was observed in experiments, i.e.$\{Mo_{72}Fe_{30}\}$ macroions do form 2D monolayers,

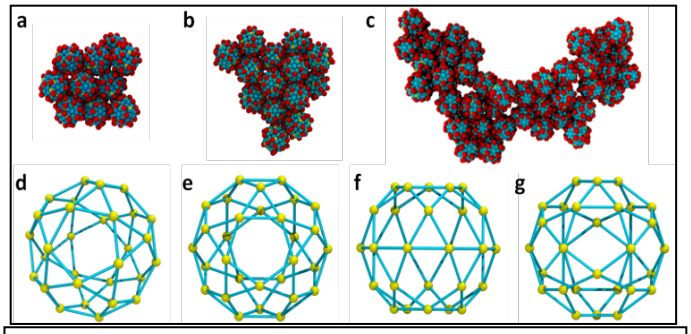

Figure 5. Self-assembly of macroions with a quasi-isotropic (icosidodecahedron shaped) charge distribution. (a) Self-assembled structure of 10 macroions. (b) After adding four macroions one by one into a. (c) 2D monolayer merged from four small monolayers as shown in a. (d) The shape of an icosidodecahedron. (e) The top view of this polyhedron when sitting on one of its pentagons on the surface. (f) The side view when sitting on one of the pentagons. (g) The side view when sitting on one of the triangles.[92]

but is contrary to our initial expectation that the charge distribution on the surface of icosidodecahedron is isotropic.

A closer look at of the charge distribution on the surface of icosidodecahedron, however, reveals a very interesting and convincing behaviour. Top and side views of the icosidodecahedron structure when it sits on one of its pentagons on a surface is shown in Figure 5e-f. The side view of the vertices shows an anisotropic charge distribution where the density of the vertices around the equator was found to be relatively higher resulting the charge density in this region to be 57% higher than the rest of the surface area[92]. In contrary to this, the charge density around the equator is about 47% lower than the rest of the surface area when the icosidodecahedron sits on one of its triangles as shown in Figure 5g. It is interesting to note that the macroions in the monolayers in Figure 5a-c align themselves along their pentagons instead of the triangles in agreement with our reasoning[92]. This exercise clearly confirmed our simulation results about the distribution of charges on the surface of macroions in solution. Putting together all our findings so far makes us believe that the charges on the macroions don't need to move far, even a slight tendency of redistributing the charges closer to the equator would lead to the formation of 2D monolayer structures. This is most feasible for macroions with highly delocalized charges such as {Mo154}.

3.4. How does the type of charge distribution on the surface of macroions we discovered from our simulation lead to a 2D monolayer formation?[92] Since electrostatic interaction mediated by counterions has been proven to be responsible for the self-assembly of macroions in solution, we focused our attention on the electric field surrounding the macroions.

Constructing the total electric field lines around the macroions as shown in Figures 6a and 6b clearly shows that the like-charged macroions repel each other in the absence of counterions (Figure 6a). After dimer formation due to the presence of counterions, electric field lines that are attractive to other macroions are observed around the dimer (Figure 6b). The electric field approach was used to explain how macroions dimerize and eventually form a stable monolayer. This was followed by use of the same approach to verify how small monolayer pieces merge into a bigger one. In order to do that, four replicas of the small monolayer

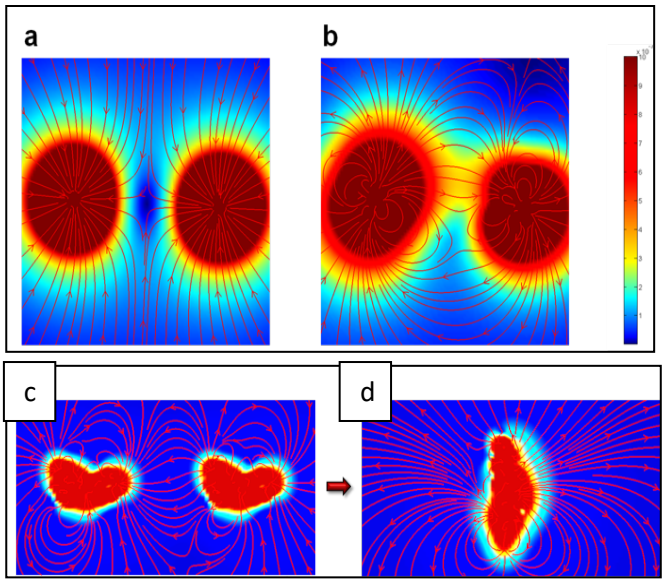

Figure 6. Electric field around a macroion or a monolayer. (a) Two single negatively charged macroions brought next to each other. (b) As in (a) but surrounded by counterions, before forming a stable dimer. (c) Two monolayers of figure 5(a) close to each other and (d) after the two monolayers have merged as one. The arrows show the direction of the field lines, and the colours manifest the strength of the electric field.

shown in Figure 5a were put in a large solution system and after running the simulation for hundreds of nanoseconds they merged with each other as shown in Figure 6d. The corresponding field lines when two of these monolayer pieces are about to merge are shown in Figure 6c, which are clearly attractive. After forming one big monolayer, the total field lines are again ready to attract other macroions or monolayers as shown in Figure 6d.

By investigating the curvature of the different monolayers in solution, we found that the monolayers are not rigidly flat, instead their curvature fluctuates most of the time. We hypothesize that the non-rigidity nature of the monolayers may allow the electric field to curve the monolayers and ultimately form the well-known blackberry structure.

3.5. Effect of Subnanometer Co-ions on Macroions Self-assembly in Solution[96]: In all the results reported above, the counterions played a crucial role in the self-assembly of macroions in solution and their role is well-understood. The role of co-ions, i.e., ions carrying the same type of charge as the macroions, in the self-assembly of macroions is relatively less explored. Logically, when the co-ions become bigger, their impact on the macroions should increase. Experiments revealed that subnanometer co-ions can significantly reduce the size of the blackberry structure[95]. When the sizes of the co-ions become comparable with the size of the original macroions, they behave like another type of macroion. In such case there are two different types of macroions coexisting in solution and they would assemble individually – by following the rule of self-recognition for macroions.[47,48] Based on these observations, the hypothesis from the experiments was that the presence of the co-ions weakens the attraction between macroions in solution.

To verify the experimental hypothesis using our CG model through simulations, the macroions and the subnanometer co-ions were represented by a 2.5 nm and a 1 nm hollow sphere, respectively, with same charge types[96]. Three systems: system 1 containing only macroions in solution, system 2 containing only co-ions in solution, and system 3 containing both co-ions and macroions in solution were simulated.

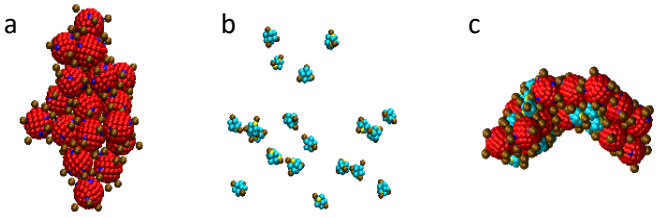

Figure 7. Self-assembly of co-ions and macroions in solution. (a) self-assembled structure of system 1 (with no co-ions), (b) co-ions do not self-assemble by themselves (system 2), and (c) macroions and co-ions self-assemble together (system 3).

As shown in Figure 7a and 7b, the macroions do self-assemble into 2D monolayer structure, as expected, while the co-ions never co-assembled even at a dimer scale and were well-dispersed in the solution. The mixture of the two, however, resulted in both the macroions and co-ions self-assembling together as shown in Figure 7c. The simulations revealed that the co-ions that are dispersed in the structure increase the distance between adjacent macroions, thus weakening the attraction between them as hypothesized based on the experimental results. Furthermore, the co-ions increase the curvature of the self-assembled monolayer significantly, as shown in Figure 7c, implying a smaller size full spherical assembly as also observed in the experiments.

These preliminary results clearly demonstrate the validity of our CG model which correctly captures that co-ions do not self-assemble by their own. Further, in accordance with the above experimental observation, the co-ions do co-assemble with macroions and result in increasing the curvature of the monolayer that ultimately forms the blackberry structure. We also found from our simulations that the co-assembled system is thermodynamically favorable and lowers the system free energy. The self-recognition behavior has not been observed in subnanometer co-ions since these co-ions cannot self-assemble by themselves to lower the system free energy. Therefore, to minimize the system free energy, the co-ions must co-assemble with macroions. When the co-ions size becomes comparable with that of the macroions, they exhibit self-recognition behavior and assemble by themselves without interfering with the macroions self-assembly.

The experimental results point to two parameters, co-ion size and long-range electrostatic interactions, to be the main players in the self-recognition process. This can be replaced by one parameter, charge density of the co-ions. Future investigation on the role of co-ions will focus on: (i) the effect of charge density of the co-ions, which can be varied by both changing the size of the co-ion and also surface charge density, on the self-recognition and self-assembly of macroions, (ii) the effect of counterions, such as monovalent, divalent and trivalent, on the self-recognition and self-assembly of macroions, and (iii) the distribution of co-ions in the co-assembly. Furthermore, information about the accurate distribution of the co-ions in the co-assembly is lacking from both experiments and simulations. In the preliminary simulation results presented in Figure 7c, the number of macroions and co-ions in the system is too small to make a conclusive statement about the co-ions distribution in the co-assembly. In the future, much larger system sizes, at least four times larger than this preliminary investigation, will be simulated to elucidate the distribution of the co-ions in the co-assembled monolayer structure.

4. Conclusions and perspectives

Our ongoing research and emergent results briefly discussed above have pointed to a promising and fruitful direction on the self-assembly behavior of macroions in solution. There are many directions for the community working on self-assembly of macroions to pursue. There remains much phenomenology to

experimentally explore. Meanwhile, molecular dynamics simulations can prove or disprove several hypotheses that have been already proposed by experiments pertaining to the self-assembly of macroions in solutions. While our recent simulation results have answered several outstanding questions related to the nature of macroions self-assembly in solution, they are just the tip of the iceberg compared to the amount of experimental data that need to be understood. Our recent simulation and experimental results from our experimental collaborator and other research groups show that the self-assembly of macroions depends on the macroionic size, charge density, and concentration. Experimental results also show that the polarity of the solvent and the valence of the counterions also determine the self-assembly behavior[97]. Furthermore, the self-assembly process can be significantly altered by covalently attaching hydrophobic molecules to the macroions. In the future, simulations are expected to conclusively explain the role played by the different components that exist in macroionic solutions.

Author Contributions

MT wrote the first draft of the manuscript, and all the authors revised the draft and approved the final version of the manuscript.

Conflicts of interest

There are no conflicts to declare.

Acknowledgements

MT gratefully acknowledges continuous support from NSF (CHE 1665284 and 2106196) for modelling the self-assembly behavior of Macroions. We thank several of Tianbo Liu's former PhD students for the experimental collaboration that led to the development of our coarse-grained model. We are particularly thankful to Jiahui Chen for several stimulating discussions and Yuqing Yang for help in designing the TOC.

Notes and references

1. A. Müller, A. Dress and F. vogtle, From Simplicity to Complexity in Chemistry - and Beyond: Part I, Vieweg: Braunschweig, Berlin, 1996.
2. C. L. Hill, Chem. Rev., 1998, **98** (1), 1-2.
3. D.-L. Long, E. Burkholder and L. Cronin, Chem. Soc. Rev., 2007, **36** (1), 105-121.
4. A. Müller, E. Diemann, C. Kuhlmann, W. Eimer, C. Serain, T. Tak, A. Knochel and P. K. Pranzas, *Chem. Commun.*, 2001, **19**, 1928-1929.
5. R. H. Baney, M. Itoh, A. Sakakibara and T. Suzuki, Chem. Rev., 1995, **95** (5), 1409-1430.
6. P. D. Lickiss and F. Rataboul, Advances in Organometallic Chemistry; F. H. Anthony, J. F. Mark, Academic Press, 2008, **57**, 1-116.
7. M. Voronkov and V. Lavrent'yev, Springer Berlin Heidelberg, 1982, **102**, 199-236.
8. M. Fujita, D. Oguro, M. Miyazawa, H. Oka, K. Yamaguchi and K. Ogura, Nature, 1995, **378** (6556), 469-471.
9. S. Leininger, M. B. Olenyuk and P. J. Stang, Chem. Rev., 2000, **100** (3), 853-908.
10. J. K. Klosterman, Y. Yamauchi and M. Fujita, Soc. Rev., 2009, **38** (6), 1714-1725.
11. D. A. Tomalia and J. M. J. Fréchet, Dendrimers and Other Dendritic Polymers John Wiley & Sons, 2002, 1-44.
12. G. M. Dykes, J. Chem. Technol. Biotechnol., 2001, **76** (9), 903-918.
13. I. Willerich, F. Gröhn, J. Am. Chem. Soc., 2011, **133** (50), 20341-20356.
14. I. Willerich, H. Ritter and F. Gröhn, J. Phys. Chem. B., 2009, **113** (11), 3339-3354.
15. M. H. Alizadeh, S. P. Harmalker, Y. Jeannin, J. Martin-Frere and M. T. Pope, *J. Am. Chem. Soc.*, 1985, **107** (9), 2662-2669.
16. A. Müller, W. Plass, E. Krickemeyer, S. Dillinger, H. Bögge, A. Armatage, A. Proust, C.Beugholt and U. Bergmann, *Chem. Int. Ed. Engl.*, 1994, **33** (8), 849-851.
17. A. Müller, E. Krickemeyer, J. Meyer, H. Bögge, F. Peters, W. Plass, E. Diemann, S. Dillinger, F. Nonnenbruch, M. Randerath and C. Menke, *Angew. Chem. Int. Ed. Engl.*, 1995, **34** (19), 2122-2124.
18. K. Wassermann, M. H. Dickman and M. T. Pope, *Angew. Chem. Int. Ed. Engl.*, 1997, **36** (13-14), 1445-1448.
19. A. Müller, E. Krickemeyer, H. Bögge, M. Schmidtmann and F. Peters, *Angew. Chem. Int. Ed.*, 1998, **37** (24), 3359-3363.
20. M. I. Khan, E. Yohannes and R. J. Doedens, *Angew. Chem. Int. Ed.*, 1999, **38** (9), 1292-1294.
21. A. Müller, S. K. Das, V. P. Fedin, E. Krickemeyer, C. Beugholt, H. Bögge, M. Schmidtmann, B and Hauptfleisch, Z. *Anorg. Allgem. Chem.*, 1999, **625** (7), 1187-1192.
22. A. Müller, S. Sarkar, S. Q. N. Shah, H. Bögge, M. Schmidtmann, P. Kögerler, B. Hauptfleisch, A. X. Trautwein and V. Schünemann, *Angew. Chem. Int. Ed.*, 1999, **38** (21), 3238-3241.
23. R. C. Howell, F. G. Perez, S. Jain, J. W. DeW. Horrocks, A. L. Rheingold and L. C. Francesconi, *Angew. Chem. Int. Ed.*, 2001, **40** (21), 4031-4034.
24. A. Müller, E. Beckmann, H. Bögge, M. Schmidtmann and A. Dress, *Angew. Chem.*, 2002, **114** (7), 1210-1215.
25. B. Botar, P. Kogerler and C. L. Hill, *Chem. Commun.*, 2005, **25**, 3138-3140.
26. S. S. Mal and U. Kortz, *Angew. Chem. Int. Ed.*, 2005, **44** (24), 3777-3780.
27. A. M. Todea, A. Merca, H. Bögge, J. van Slageren, M. Dressel, L. Engelhardt, M. Luban, T. Glaser, M. Henry and A. Müller, *Angew. Chem. Int. Ed.*, 2007, **46** (32), 6106-6110.
28. C. Schäffer, A. Merca, H.Bögge, A. M. Todea, M. L.Kistler, T. Liu, R. Thouvenot, P. Gouzerh and A. Müller, *Angew. Chem. Int. Ed.*, 2009, **48** (1), 149-153.
29. G. F. Tourne, C. M. Tourne, *In Polyoxometalates: from Platonic Solids to Anti-retroviral Activity*,A. Müller, M. T. Pope, Eds. Dordrecht: Kluwer, 2014.
30. M. Tominaga, K. Suzuki, T. Murase and M.Fujita, *J. Am. Chem. Soc.*, 2005, **127** (34), 11950-11951.
31. Y. Nishioka, T. Yamaguchi, M. Yoshizawa and M. Fujita, *J. Am. Chem. Soc.*, 2007, **129** (22), 7000-7001.
32. T. Liu, *J. Am. Chem. Soc.*, 2002, **125** (2), 312-313.
33. T. Liu, *J. Am. Chem. Soc.*, 2002, **124** (37), 10942-10943.
34. T. Liu, E. Diemann, H. Li, A. W. M. Dress and A. Müller, *Nature*, 2003, **426** (6962), 59-62.

35. S. A. Eghtesadi, F. Haso, M. A. Kashfipour, R. S. Lillard and T. Liu, *Chem. Eur. J.*, 2015, **21**(51), 18863-18863.
36. M. L. Kistler, A. Bhatt, G. Liu, D. Casa and T. Liu, *J. Am. Chem. Soc.*, 2007, **129** (20), 6453-6460.
37. J. Zhang, B. Keita, L. Nadjo, I. M. Mbomekalle and T. Liu, *Langmuir*, 2008, **24** (10), 5277-5283.
38. T. Liu, *Langmuir*, 2009, **26** (12), 9202-9213.
39. P. P. Mishra, J. Pigga and T. Liu, *J. Am. Chem. Soc.*, 2008, **130** (5), 1548-1549.
40. T. Liu, B. Imber, E. Diemann, G. Liu, K. Cokleski, H. Li, Z. Chen and A. Müller, *J. Am. Chem. Soc.*, 2006, **128** (49), 15914-15920.
41. J. M. Pigga, M. L. Kistler, C.-Y. Shew, M. R. Antonio and T. Liu, *Angew. Chem. Int. Ed.*, 2009, **48** (35), 6538-6542.
42. J. Zhang, T. Liu, S. S. Mal and U. Kortz, *Eur. J. Inorg. Chem.*, 2010, **20**, 3195-3200.
43. G. Liu, Y. Cai and T. Liu, *J. Am. Chem. Soc.*, 2004, **126** (51), 16690-16691.
44. M. L. Kistler, K. G. Patel and T. Liu, *Langmuir*, 2009, **25** (13), 7328-7334.
45. J. M. Pigga, J. A. Teprovich, R. A. Flowers, M. R. Antonio and T. Liu, *Langmuir*, 2010, **26** (12), 9449-9456.
46. J. Zhang, D. Li, G. Liu, K. J. Glover and T. Liu, *J. Am. Chem. Soc.*, 2009, **131** (42), 15152-15159.
47. P. Yin, J. Zhang, T. Li, X. Zuo, J. Hao, A. M.Warner, S. Chattopadhyay, T. Shibata, Y. Wei and T. Liu, *J. Am. Chem. Soc.*, 2013, **135** (11), 4529-4536.
48. T. Liu, M. L. K. Langston, D. Li, J. M. Pigga, C. Pichon, A. M. Todea and A. Müller, *Science*, 2011, **331** (6024), 1590-1592.
49. A. Togo, I. Tanaka, K. Murase, T. Yamamoto, T. Suga and E. Matsubara, *Mater. Trans.*, 2004, **45** (7), 1982-1986.
50. A. J. Bridgeman and G. Cavigliasso, *Polyhedron*, 2002, **21** (21), 2201-2206.
51. A. J. Bridgeman and G. Cavigliasso, *J. Phys. Chem. A*, 2003, **107** (34), 6613-6621.
52. A. J. Bridgeman and G. Cavigliasso, *J. Phys. Chem. A*, 2003, **107** (22), 4568-4577.
53. D. G. Musaev, K. Morokuma, Y. V. Geletii and C. L. Hill, *Inorg Chem*, 2004, **43** (24), 7702-7708.
54. D. Zhang, Z. Dou, T. Zhang, L. K. Yan and Z. M. Su, *Chem J Chinese U*, 2011, **32** (11), 2613-2617.
55. M. R. S. A. Janjua, Z. Su, M. W. Guan, A. Irfan, S. Muhammad and M. Iqbal, *Can. J. Chem.*, 2010, **88** (5), 434-442.
56. X. Lopez and J. M. Poblet, *Inorg Chem*, 2004, **43** (22), 6863-6865.
57. S. A. Borshch, *Inorg Chem*, 1998, **37** (12), 3116-3118.
58. J. M. Maestre, X. Lopez, C. Bo, J. M. Poblet and N. Casan-Pastor, *J. Am. Chem. Soc.*, 2001, **123** (16), 3749-3758.
59. X. Lopez, J. M. Maestre, C. Bo and J. M.Poblet, *J. Am. Chem. Soc.*, 2001, **123** (39), 9571-9576.
60. X. Lopez, C. Bo and J. M. Poblet, *J. Am. Chem. Soc.*, 2002, **124** (42), 12574-12582.
61. A. J. Bridgeman and G. Cavigliasso, *J. Chem. Soc., Dalton trans.*, 2002, **10**, 2244-2249.
62. C. Baffert, J. F. Boas, A. M. Bond, P. Kogerler, D. L. Long, J. R. Pilbrow and L. Cronin, *Eur. J. Chem.*, 2006, **12** (33), 8472-8483.
63. L. Vila-Nadal, S. G. Mitchell, D. L. Long, A. Rodriguez-Fortea, X. Lopez, J. M. Poblet and L. Cronin, *Dalton Trans.*, 2012, **41** (8), 2264-2271.
64. R. Tsunashima, D. L. Long, T. Endo, S. Noro, T. Akutagawa, T. Nakamura, R. Q. Cabrera, P. F. McMillan, P. Kogerler and L. Cronin, *Phys. Chem. Chem. Phys.*, 2011, **13** (16), 7295-7297.
65. F. Q. Zhang, X. M. Zhang, H. S. Wu, Y. W. Li and H. J. Jiao, *J. Phys. Chem. A*, 2007, **111** (9), 1683-1687.
66. H. El Moll, B. Nohra, P. Mialane, J. Marrot, N. Dupre, B. Riflade, M. Malacria, S. Thorimbert, B. Hasenknopf, E. Lacote, P. A. Aparicio, X. Lopez, J. M. Poblet and A. Dolbecq, *Eur. J. Chem.*, 2011, **17** (50), 14129-14138.
67. A. Lewis, J. A. Bumpus, D. G. Truhlar and C. J. Cramer, *J. Chem. Educ.*, 2004, **81** (4), 596-604.
68. D. G. Allis, E. Burkholder and J. Zubieta, *Polyhedron*, 2004, **23** (7), 1145-1152.
69. F. Q. Zhang, H. S. Wu, X. F. Qin, Y. W. Li and H. J. Jiao, *J. Mol. Struc-Theochem*, 2005, **755** (1-3), 113-117.
70. C. Bo and P. Miro, *Dalton Trans.*, 2012, **41** (33), 9984-9988.
71. L. K. Yan, X. Lopez, J. J.Carbo, R. Sniatynsky, D. C. Duncan and J. M. Poblet, *J. Am. Chem. Soc.*, 2008, **130** (26), 8223-8233.
72. F. Q. Zhang, W. Guan, L. K. Yan, Y. T. Zhang, M. T. Xu, E. Hayfron-Benjamin and Z. M. Su, *Inorg Chem*, 2011, **50** (11), 4967-4977.
73. J. R. Black, M. Nyman and W. H. Casey, *J. Am. Chem. Soc.*, 2006, **128** (45), 14712-14720.
74. D. L. Long, P. Kogerler, L. J. Farrugia and L. Cronin, *Dalton Trans.*, 2005, **8**, 1372-1380.
75. X. Lopez, J. A. Fernandez and J. M. Poblet, *Dalton Trans.*, 2006, **9**, 1162-1167.
76. X. Lopez, C. Bo and J. M. Poblet, *Inorg Chem*, 2003, **42** (8), 2634-2638.
77. A. J. Bridgeman and G. Cavigliasso, *Inorg Chem*, 2002, **41** (7), 1761-1770.
78. A. J. Bridgeman and G. Cavigliasso, *J. Phys. Chem. A*, 2002, **106** (25), 6114-6120.
79. F. Q. Zhang, H. S. Wu, Y. Y. Xu, Y. W. Li and H. J. Jiao, *J. Mol. Model.*, 2006, **12** (5), 551-558.
80. X. Lopez, J. J. Carbo, C. Bo and J. M.Poblet, *Chem. Soc. Rev.*, 2012, **41** (22), 7537-7571.
81. M. Grabau, J. Forster, K. Heussner and C. Streb, *Eur. J. Inorg. Chem.*, 2011, **11**, 1719-1724.
82. Y. G. Chen, L. K. Yan, X. R. Hao, K. Liu, X. H. Wang and P. P. Lu, *Inorg. Chim. Acta*, 2006, **359** (8), 2550-2554.
83. J. L. Zhang, W. P. Wu and Z. X. Cao, *J. Mol. Struc-Theochem*, 2005, **756** (1-3), 79-85.
84. D. Laurencin, A. Proust and H. Gerard, *Inorg. Chem.*, 2008, **47** (17), 7888-7893.
85. K.Tsujimichi, M. Kubo, R. Vetrivel and A. Miyamoto, *J. Catal.*, 1995, **157** (2), 569-575.
86. B. Torok, M. Torok, M. Rozsa-Tarjani, I. Palinko, L. I. Horvath, I. Kiricsi and A. Molnar, *Inorg. Chim. Acta*, 2000, **298** (1), 77-83.
87. X. Lopez, C. Nieto-Draghi, C. Bo, J. B. Avalos and J. M. Poblet, *J. Phys. Chem. A*, 2005, **109** (6), 1216-1222.
88. F. Leroy, P. Miro, J. M. Poblet, C. Bo and J. B. Avalos, *J. Phys. Chem. B*, 2008, **112** (29), 8591-8599.
89. A. Chaumont and G. Wipff, *Phys. Chem. Chem. Phys.*, 2008, **10** (46), 6940-6953.
90. A. Chaumont and G. Wipff, *C. R. Chim.*, 2012, **15** (2-3), 107-117.
91. Z. N. Liu, T. B. Liu and M. Tsige, *Sci. Rep.*, 2016, **6**, 26595.
92. Z. N. Liu, T. B. Liu and M. Tsige, *Sci. Rep.*, 2018, **8**, 13076.
93. S. O. Yesylevskyy, L. V. Schafer, D. Sengupta, and S. J. Marrink. *Plos Comput Biol*., 2010, **6** (6), 1-17.

94. Y. Yang, Y. Zhou, J. Chen, T. Kohlgruber, T. Smith, B. Zheng, J. E. Szymanowski, P. C. Burns, and T. Liu., *J. Phys. Chem. B*, 2021, **125** (44), 12392-12397.
95. Y. Yang, P. Rehak, T. Xie, Y. Feng, X. Sun, J. Chen, H. Li, P. Kral, and T. Liu. *ACS Appl. Mater. Interf.*, 2020, **12**(50), 56310-56318.
96. J. Chen, K. Qian, K. Xiao, J. Luo, H. Li, T. Ma, U. Kortz, M. Tsige, and T. Liu, *Langmuir*, 2020, **36**(35), 10519-10527.
97. J. He, H. Li, P. Yang, F. Haso, J. Wu, T. Li, U. Kortz and T. Liu, *Eur. J. Chem.*, 2018, **24**, 3052-3057.